CHARACTERIZATION OF THE PORE SPACE ACCESSED BY THE NON-WETTING PHASE DURING CONSTANT RATE INJECTION AT THE BREAKTHROUGH CAPILLARY PRESSURE

J.D. Smith and I. Chatzis
Department of Chemical Engineering, University of Waterloo, Ontario, Canada

ABSTRACT

The breakthrough capillary pressure is an important macroscopic property of porous media that is used to predict permeability and to correlate capillary pressure curves. The breakthrough capillary pressure in mercury porosimetry is identified as the pressure corresponding to about 10 - 20% non-wetting phase saturation. In the literature, it is identified as the pressure corresponding to the point of inflection in the drainage capillary pressure curve. A new method of measuring the breakthrough capillary pressure has been developed, involving a constant rate injection of the non-wetting phase as opposed to constant injection pressure and was reported at the SCA 2002 meeting. The scope of this paper is to report the methodology used for characterization of pore space accessed by the non-wetting phase as it penetrates into a porous medium at constant injection rate. The pressure trace recorded near the face of injection using a data acquisition system and the volume of the non-wetting phase injected as a function of time are utilized for the characterization of pore throat sizes and the associated pore volume involving several pore bodies accessed in the pore accessibility process. The injection pressure-versus-time plot reveals pressure fluctuations that are associated with menisci positions in pore throats and in pore bodies. The local maximum in pressure represents penetration in a pore throat and the local minimum value in pressure represents conditions of a meniscus advancing into pore bodies and pore throats of larger size. The transformation of the pressure versus time data into volume accessed versus pore size data enables the determination of pore space accessibility associated with this backbone of pore space. The pore volume fraction of wetting phase displaced at gas breakthrough is correlated with the structure of the porous medium. The more homogeneous the sample is, the greater is the fraction of wetting phase produced at breakthrough capillary pressure.

INTRODUCTION

Mercury porosimetry is normally performed by increasing the pressure in increments, maintaining that pressure and recording the change in non-wetting phase volume injected into a porous sample. The work of Yuan and Swanson [1] introduced a new technique to porosimetry, termed APEX, where mercury was instead injected at constant rate. They showed that APEX porosimetry was able to produce more information about pore space

characterization by separating the total capillary pressure curve into two parts: the rison capillary pressure curve and the subison capillary pressure curve [1]. Since the work of Yuan and Swanson, others have explored the uses of APEX, including Toledo et al. [2], who studied the effects of sample size on APEX response, and Knackstedt et al. [3], who used APEX to demonstrate the presence of correlated heterogeneity in reservoir rocks even at the pore scale.

The breakthrough capillary pressure of a porous medium is an important macroscopic pore structure parameter that can be used to predict absolute permeability and correlate capillary pressure curves via the reduced capillary pressure curves concept [4]. It is properly defined as the capillary pressure required by the non-wetting phase to penetrate through a given sample indefinitely. Because APEX porosimetry involves full invasion of all pore space until the non-wetting phase saturation approaches 100%, the accessibility of pore space at the breakthrough capillary pressure can not be directly obtained from the pressure trace. Smith et al. [5] introduced an adaptation of APEX porosimetry where air could be injected through a brine-saturated media at constant rate to obtain the breakthrough capillary pressure; a modification to this technique was made to measure the breakthrough capillary pressure of glass micromodels using mercury, with air acting as the wetting phase. By invading a porous medium only to breakthrough capillary pressure conditions, more information about the pore space that contributes most to permeability can be obtained. The pores invaded by the non-wetting phase at breakthrough conditions represent the pore space at the percolation threshold, to which we wish to pay particular attention in this paper.

Yuan and Swanson [1] proposed a terminology to label the pressure response to events that occur during the invasion of a porous medium under constant injection flow rate conditions. They termed a rison as increasing capillary pressure to previously unattained levels and a rheon as a sudden drop in capillary pressure, associated with the global drainage of mercury from regions of high capillary pressure in the sample (i.e. interfaces at pore throats) that is instantaneously redistributed into a region of low capillary pressure (i.e. interfaces in a pore body) [1]. A subison involves increasing capillary pressure immediately following a rheon to levels that have been obtained previously. Furthermore, Yuan and Swanson termed a subison pore system as a sequence involving only rheon and subisons [1]. All four events are shown in Figure 1 for clarification, with the subison pore systems labeled as 'A' and 'B'. For the purpose of this work, a modification is made to the terminology explained above. Whereas a subison pore system is normally taken to be the sequence of events occurring between two risons, we identify any events between two rises in capillary pressure (either subisons or risons) to be a subison pore system. In this way, every large subison pore system composed of multiple events and representing the invasion of multiple pores is broken down into successively smaller and smaller sequences, until at last there are only individual pore invasion events remaining. This identification is similar to the concept of a *pore segment* introduced by Toledo et al. [2], which was defined as the pore space filled after one rheon and immediately before the next rheon. However, our classification system involves pore

systems that can encompass other smaller pore systems, as well as individual pore systems involving a single rheon. According to the Yuan and Swanson terminology, there are only two subison pore systems present in Figure 1. With the modified classification scheme however, there are now six, with the extra four labeled as 'C', 'D', 'E' and 'F' and marked by dotted rather than dashed lines.

Using the modified classification scheme, analysis of pore space was conducted using both computer simulated pore networks (featuring either correlated or uncorrelated pore indices) and experiments involving the invasion of mercury into glass micromodels with a pore size distribution of pore bodies and pore throats. Both results are reported and discussed, and comparisons drawn where appropriate. For brevity, the term "subison pore system" may, from time to time, be abbreviated to SPS in ensuing sections of this work.
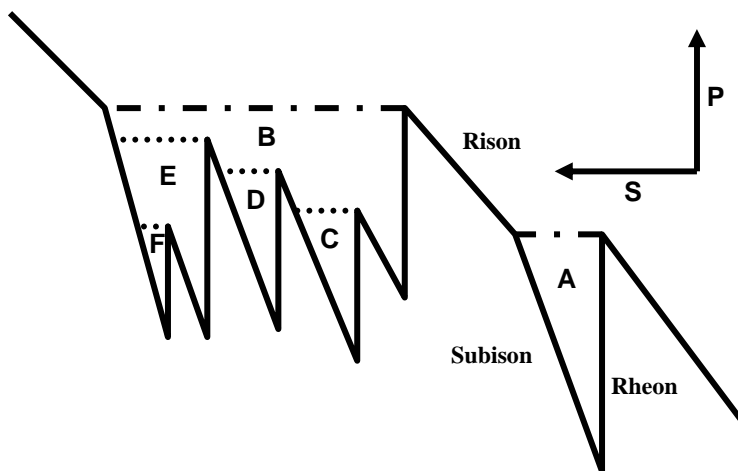
Figure 1: Illustration of Subison Pore Systems

SIMULATION AND EXPERIMENTAL ASPECTS
Pore Network Simulation
A Visual C++ based program was constructed to simulate the invasion of a non-wetting phase into a 2-D pore network. The network was a site-lattice type, with each node representing a pore body and assigned a pore index number j (j = 1, 2, …50) corresponding to a capillary pressure, which in turn represents the average of a capillary pressure range . The index for a bond between two nodes represents a pore throat and it was assumed that the bond index is correlated with the largest index of the two nodes it connects. For example, to penetrate into a pore of index j =15 from a pore of index j =2, the bond connecting them has index j =15 and the capillary pressure required to invade into the pore of index 15 from a pore of index 2 is that corresponding to invading pore throats of index 15. Details of invasion percolation in bond correlated site percolation type of network models are given elsewhere [4]. Two lattice types were used: uncorrelated (500 by 500 nodes) and spatially correlated (500 by 500 nodes). For the

latter, a direct Fourier transform method was used to impose exponential correlations among node indices with correlation length equal to 5 and 8 lattice sites (see Robin et al. [5]). The co-ordination number of all lattices was 4. Initial invasion into the pore lattices occurred from a single node, which was required as input by the program, and consistently set as the pore of lowest capillarity on the 'top' or entrance face of the lattice. The program then proceeded to invade pore sites according to invasion percolation theory, i.e. in order of highest to lowest of positive potential sites. Invasion potential, Φ, between two nodes i and j, was calculated via the following equation,

$$\Phi_{ij} = P - P_{ij}^c + R_N(\ )$$ [1]

where P is in the injection pressure taken as input by the program. P^c_{ij} is a pressure value set to the greater of the two capillary pressures that correspond to the index numbers of nodes i and j, as explained earlier. R_N is a random number that is added to all calculated potentials to ensure that having nodes of high capillary pressure does not necessarily mean having multiple invasions (since high index number nodes control potential, without R_N, all surrounding nodes of lower index number have the same potential for invasion and are therefore invaded simultaneously by the simulation program). Its magnitude is such that it can not alter the decision to invade nodes out of order (i.e. its maximum value is smaller than the difference in capillary pressure between two successive pore indices). R_N can take on one of 10,000 possible values, and therefore, it is still possible that multiple pore invasions can occur simultaneously, since there is a chance high index number nodes will be assigned the same value of R_N. However, the invasion process is biased towards single pore invasion.

The program was set to stop if all potentially accessible sites (i.e. $\Phi_{ij} > 0$) had been invaded, or one of two preset conditions took place: (a) breakthrough occurred, i.e. any pore on the exit face of the lattice was penetrated or (b) all sites within the lattice had been invaded. In this way, the program could run in either true APEX mode (full invasion) or breakthrough mode, stopping once a lattice-spanning, continuous non-wetting phase had been established at the percolation threshold condition. Input pressure was always set according to the type of test: for full invasion, it was set to allow for invasion of any site, up to pore index 50. For partial invasion, the pressure was set to just above the percolation threshold. For the case of uncorrelated site percolation, this corresponds to allowing pores of index 1 to 30 (site percolation probability = 0.6) to be invaded. Output from the simulation program included a visual representation of the breakthrough pathway (if applicable) and a sequence of numbers representing the pore index values of invaded sites in the actual order they were accessed by the non-wetting phase. This data set was then sent as input to a MatLab-based analysis program that broke down the chain of numbers into numerical representations of subison pore systems. Analysis was done as follows: although pore index numbers are assigned to every pore body, their corresponding values of pressure actually represent the capillary pressure required to be exceeded in the connecting pore throats. Thus, when analogy to

experimental systems is made, the pore index values represent the capillary pressure sensed immediately before a rheon event occurs, i.e. just before the site is invaded by the non-wetting phase. A particular subison pore system is then taken as the time between encountering one pore index number and another index number of an equal or higher index value. Subison pore systems are classified by both their size (in terms of number of pores) and their controlling value (i.e., the pore index number at which the pore system began). To further clarify, consider the following sequence of numbers, representing a chain of pore index values from invaded sites:

$$24 \quad 5 \quad 3 \quad 12 \quad 8 \quad 6 \quad 7 \quad 8 \quad 12 \quad 15 \quad 24$$

Because of the modified classification scheme, there are always as many subison pore systems as there are invaded sites. However, the pore systems will vary drastically in size. The first pore system encountered is of index 24, and it is 10 pores in size, since there are nine pores of smaller capillary pressure between the two values of 24. The next subison pore system is of index 5 and is two pores in size (since 12 is higher than 5, and there is one pore between 5 and 12). Note that this subison pore system is located within the first one of 24; under the new classification scheme, this is possible, since the pore space is divided and subdivided until it has reached its smallest units. For instance, the next subison pore system is of index 3, and this is only one pore in size. That is because there are no pores lower than 3 following the initial site.

Multiple subison pore systems are tracked simultaneously with the MatLab analysis program. During the program, several pieces of information are also recorded. Firstly, the number of subison pore systems controlled by a particular pore index number are counted. Second, the average size of the pore systems for each index number are calculated. Lastly, every subison pore system is classified and sorted into one of six bins based on its size (in terms of number of pores contained within it). The size ranges are shown in Table 1. Sorting the subison pore systems by size enables the calculation of two pieces of information.
1. The distribution of subison pore system sizes for a given pore index number can be calculated. In other words, it can be shown what fraction of pore systems controlled by index 'j' are within a certain size range.
2. The distribution of pore indices contributing to subison pore systems of a given size can be calculated. In other words, what fraction of pore systems of a given size are controlled by pore index 'j' (i.e. controlled by pores corresponding to a particular capillary pressure range).

Table 1: Bin Ranges for Storing Subison Pore Systems

Bin 1	1 - 5 pores	**Bin 4**	21 - 50 pores
Bin 2	6 - 10 pores	**Bin 5**	51 - 100 pores
Bin 3	11 - 20 pores	**Bin 6**	101 + pores

Micromodel Experiment

To test the new classification scheme and show that it can be applied to real-life experiments, a modified APEX test was conducted on a glass micromodel. Mercury was injected at a constant rate of 6.0 x 10^{-4} mL/min into the micromodel and the pressure response with time recorded using a pressure transducer connected to a data acquisition system. The experimental apparatus and procedure are exactly that used in previous experiments reported by Smith et al. [6].

Analysis of the experimental data points on the pressure trace was done manually. Pore events that were resolvable (because of limitations on pressure transducer sensitivity, some smaller pore events are inevitably lost as signal noise) had their corresponding pressure and volume recorded. The capillary pressure range over the entire experiment was subdivided into twenty equal smaller ranges, each of which was assigned a pore index number; all subison pore systems were then assigned to their appropriate pore index. Furthermore, pore systems were classified by volume into six bins representing a range of pore volumes. Bin details are shown in Table 2.

Table 2: Bin Ranges for Micromodel Experiment

Bin 1	0 - 0.25 µL	Bin 4	> 1.0 - 2.5 µL
Bin 2	> 0.25 - 0.5 µL	Bin 5	> 2.5 - 5.0 µL
Bin 3	> 0.50 - 1.0 µL	Bin 6	> 5.0 µL

RESULTS AND DISCUSSION

Pore Network Simulation Results

Figure 2 shows the relationship between average subison pore system size and pore index number for both correlated and uncorrelated lattices (the data represent typical results). For the uncorrelated lattice, the average size of subison pore systems increases smoothly, from a limiting value of one pore at index 1 and increasingly rapidly as the percolation threshold (index 30) is approached. This smooth trend is not observed in either of the correlated lattices; instead, local maxima exist in between lowest pore index and the highest pore index. In media featuring correlation between adjacent nodes, clustering of similar sized pores occurs and therefore even for lower pore index numbers, there is a significant chance that large subison pore systems may exist. For uncorrelated media, large subison pore systems are encountered in statistically significant quantities only at much higher pore index number. Note that there is also similarity between all three media: as their respective percolation thresholds are approached, the average size of subison pore system increases very rapidly. This marked jump in size occurs at a lower pore index number for the two correlated media than the uncorrelated media, since their percolation thresholds are lower.

Figure 3 is similar to Figure 2 except that it shows the full invasion of the networks (true APEX). The left portion of the graph (before the various percolation thresholds) is similar to the case for partial invasion, with the correlated media featuring local maxima and the uncorrelated medium showing smooth growth. On the right side of the plot (i.e.

past the percolation threshold), the average size of subison pore systems drops very sharply and for pore index greater than 35, the average SPS size for all media is essentially unity. This is the result of increased pore accessibility once the percolation threshold has been exceeded. At this point, a large portion of a medium has been invaded, and most pores can be reached directly by the non-wetting phase. This leads to significant single-pore type invasion, reducing the average subison pore system size to one. There are some differences between the results from correlated and uncorrelated lattices. Firstly, the trends for the correlated media are not smooth, whereas the uncorrelated media is. Second, the sharp drop in average subison pore system size occurs earlier in the correlated media, since their percolation thresholds are reached earlier.
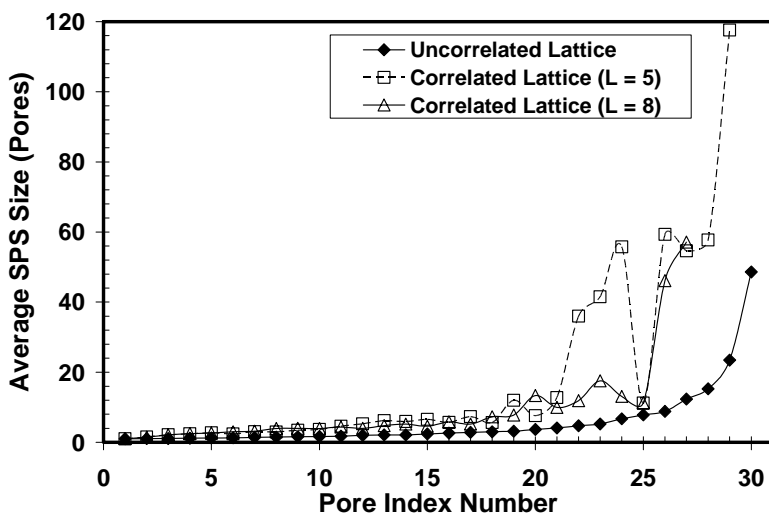
Figure 2: Average SPS Size vs. Pore Index Number (Partial Invasion)
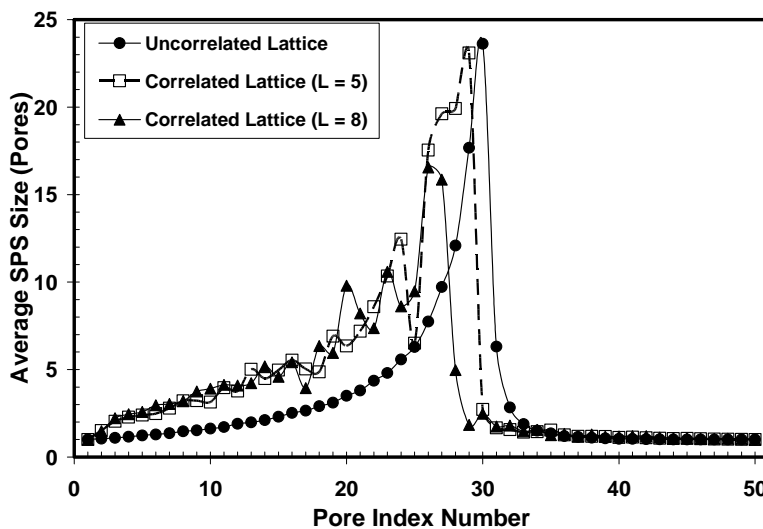
Figure 3: Average SPS Size vs. Pore Index Number (Full Invasion)

Figure 4 shows the distribution of subison pore system sizes for every pore index number in the uncorrelated lattice. Here, relative number frequency is defined as the number of subison pore systems of index j found in a given size range (i.e. bin k) divided by the total number of subison pore systems of index j over all sizes (i.e. bins 1 – 6). Until pore index 8, all pore systems are within bin 1, or 1 to 5 pores in size. After that, other size ranges begin to play a more important role in the composition of subison pore systems of a given pore index, until about pore index 25, where the contribution of smaller (1 – 5 pore) pore systems begins to increase again. Note that subison pore systems of larger size (i.e. higher bin number) begin to appear only at successively larger and larger pore index numbers.
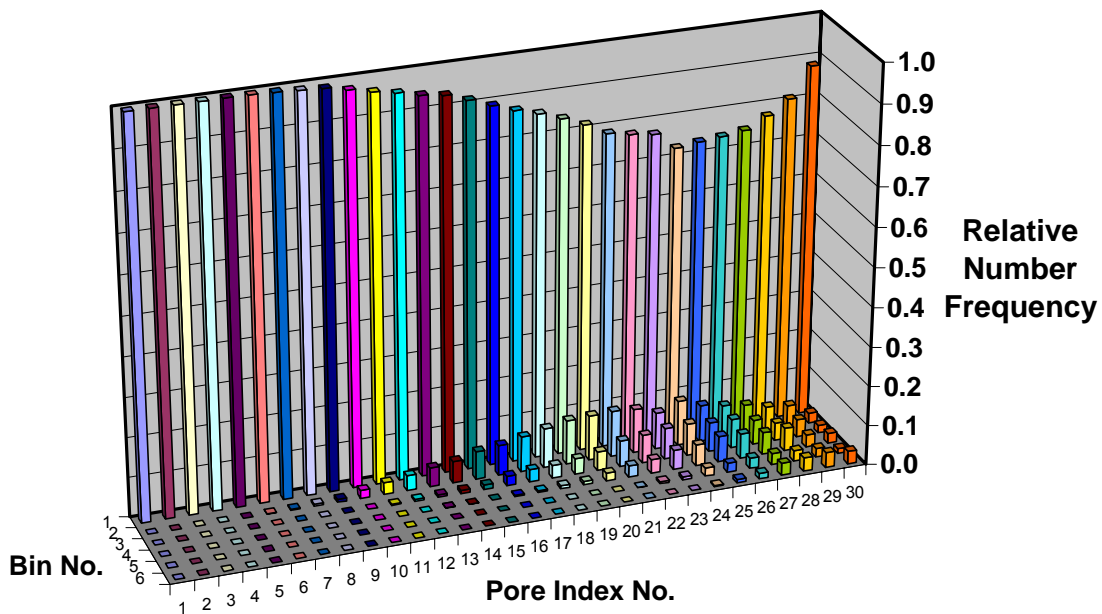
Figure 4: Distribution of SPS Sizes (Uncorrelated Lattice)

Figures 5a and 5b show the cumulative relative fraction of subisons in each size range for each lattice type. Relative fraction is defined as the number of subison pore systems of index j in a given size range, bin k, divided by the total number of subison pore systems in that size range (encompassing all pore indices). In other words, it quantifies what fraction of subison pore systems of a certain size are controlled by pores of a given capillary pressure. There are notable differences between Figure 5a and Figures 5b. For instance, the range over which large subison pore systems (i.e. bin 6) are found is vary narrow for the uncorrelated lattice (none are encountered until about pore index 23) whereas the distribution is broad for the correlated lattices (some subison pore systems appear at index 4). Furthermore, for systems of size greater than 5 pores (i.e. bins 2 – 6), approximately 90% or more are encountered by pore indices up to and including the percolation threshold for the uncorrelated lattice. On the other hand, for the correlated lattices, only the top two subison pore size classes (bins 5 and 6) are over 90% accounted

for by the percolation threshold.   Generally, the trend shows that the distributions become broader by introducing correlated heterogeneity, and also become broader as the correlation length is increased (contrast bin 6 in Figures 5b). Overall, these two figures show that the most important portion of the pore space in terms of accessibility is encountered at pressures up to an including the percolation threshold. This pore space, which essentially composes the breakthrough pathway, represents the majority of the subison pore systems of relatively large volume.
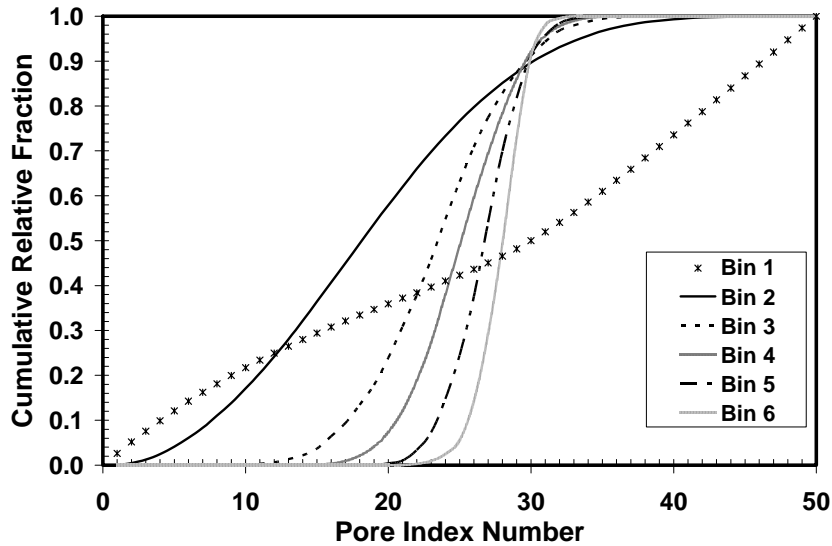
Figure 5a: Cumulative SPS Size Distribution (Uncorrelated Lattice)
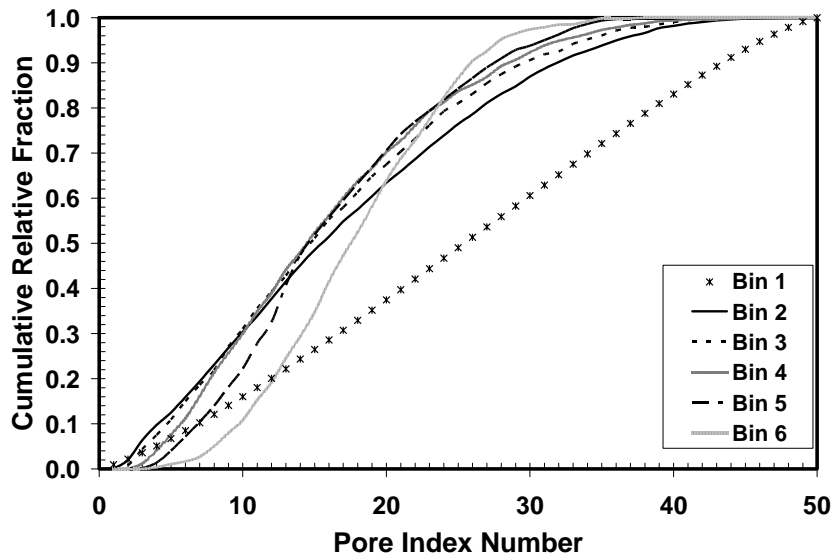
Figure 5b: Cumulative SPS Size Distribution (Correlated Lattice, L = 5)

Experimental Results

The trace of pressure versus time for the micromodel experiment is shown in Figure 6. For the purposes of perspective, the first large subison pore system shown in Figure 6, (beginning at approximately 7 minutes and ending at approximately 24 minutes) represents an injection volume of 9.74 μL or, based on experimental visualization, the filling of about 200 pores. Figure 7 is an examination of the resolvable, experimental subison pore systems based on the analysis scheme detailed in previous sections. When compared to the simulation results, the trend in Figure 7 more closely resembles the correlated lattice results than the uncorrelated lattice results, since the data exhibit local maxima and minima. Figure 8 is the equivalent of Figure 5 but applied to the experimental data. Due to the limited amount of data collected, the trends are not smooth, and the data represent only partial (breakthrough) invasion, unlike the data presented in Figure 5. For comparison purposes however, the experimental data resemble the correlated lattices better since the mid-range bins (2 – 4) behave similarly, as they do in Figure 5b.

A truly fair comparison between experimental and simulated results is not possible. Firstly, subison pore system size is defined in terms of number of pores for the simulation results, and therefore the volume based SPS sizes reported for the experimental results can only be directly compared assuming all pores in the simulated lattice are of equal volume. This is, of course, a poor assumption. Second, the resolvability of the experiment is not adequate to count all of the subison pore systems; the smaller sized systems are simply lost as signal noise and thus are not counted. Lastly, the number of invasion events in the micromodel experiment is very small compared to the number of invasion events realized during the penetration of the simulated lattices. Thus, the statistics of the experimental may be skewed by the fact that there are less data available (the micromodel contained about 3,200 pores total).
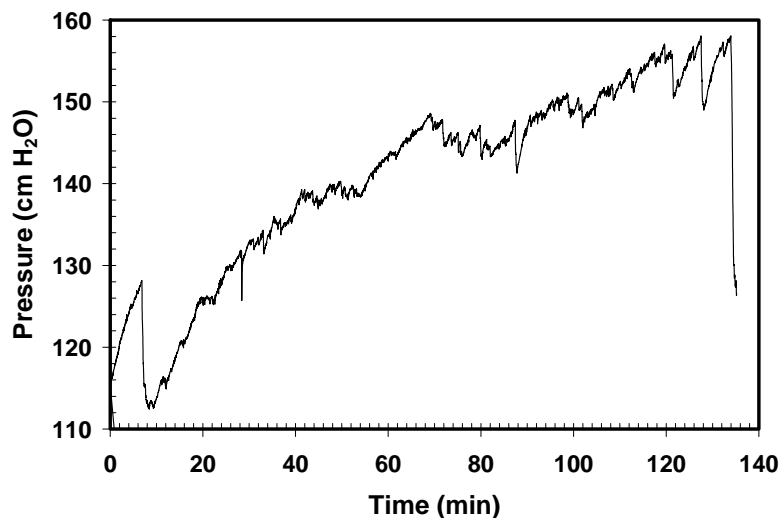
Figure 6: Pressure Trace from Mercury-Air Micromodel Experiment
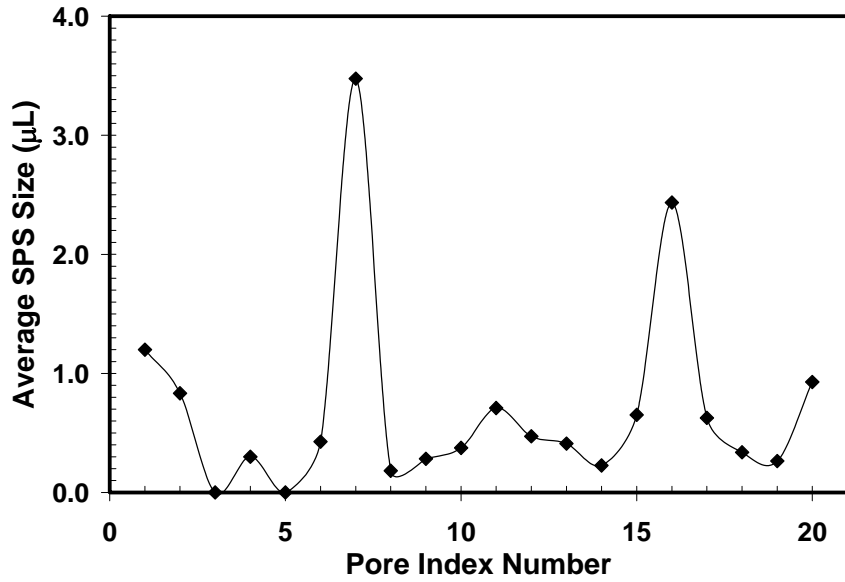
Figure 7: Average SPS Size for Micromodel Experiment
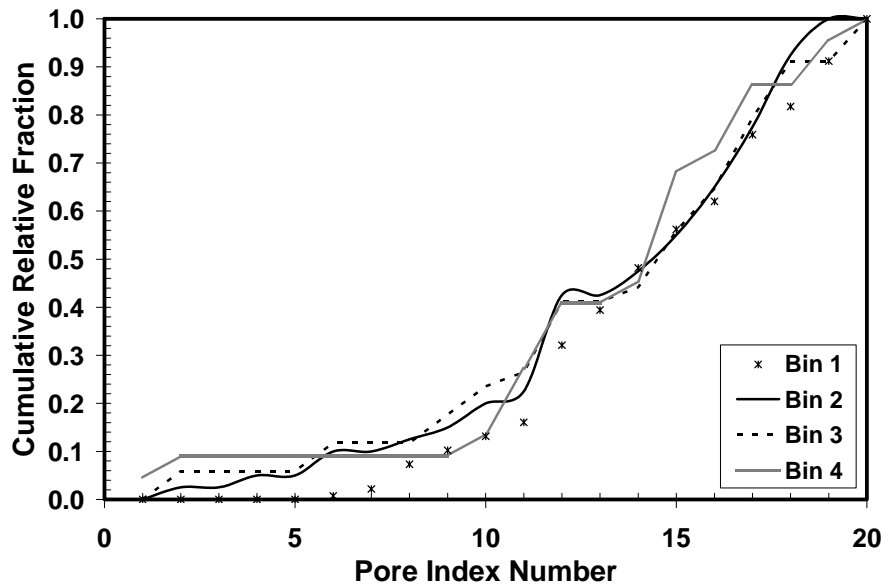
Figure 8: Cumulative SPS Size Distribution (Micromodel Experiment)

CONCLUSIONS

- A new scheme of analysis of the pressure trace during constant rate injection of mercury at breakthrough capillary pressure into a porous medium was developed.
- Concepts were applied using 2-D network models of co-ordination number 4 with and without correlated structure in distributing pore body sizes. It was found that very large sized subison pore systems at breakthrough capillary pressure involve pore of entry sizes close to the breakthrough capillary size in uncorrelated network models, while for correlated pore networks, the range of pore body and throat sizes involved is much greater.
- Experiments with micromodels have shown that the average subison pore system size resembles features seen in correlated networks.

ACKNOWLEDGEMENTS

REFERENCES

1. Yuan, H.H. and B.F. Swanson. "Resolving Pore Space Characteristics by Rate-Controlled Porosimetry," *SPE Formation Evaluation*, **4**, 1989. p.p. 17 – 24.
2. Toledo, P.G., L.E. Scriven and H.T. Davis. "Pore-Space Statistics and Capillary Pressure Curves From Volume-Controlled Porosimetry," *SPE Formation Evaluation*, **9**(1), 1994. p.p. 46-54.
3. Knackstedt, M.A., A.P. Sheppard and W.V. Pinczewski. "Simulation of Mercury Porosimetry on Correlated Grids: Evidence for Extended Correlated Heterogeneity at the Pore Scale in Rocks," *Physical Review E*, **58**(6), 1998.
4. Chatzis, I. and F.A.L. Dullien. "The Modelling of Mercury Porosimetry and the Relative Permeability of Mercury in Sandstones Using Percolation Theory," *International Chemical Engineering*, **25**(1), 1985. p.p. 47 – 66.
5. Robin, M.J.L., A.L Gutjahr, E.A. Sudicky and J.L. Wilson. "Cross-Correlated Random-Field Generation with the Direct Fourier Transform Method," *Water Resources Research*, **29**(7), 1993. p.p. 2385-2397.
6. Smith, J.D., I. Chatzis and M.A. Ioannidis. "A New Technique for Measuring the Breakthrough Capillary Pressure," Proceedings of the SCA 2002 Annual International Symposium. Sep. 22 – 26, Monterey, CA. Paper No. 2002-40.